

A Co-pyrolysis Method to Boron Nitride Nanotubes at Relative Low Temperature

Liqiang Xu,^{†,‡} Yiya Peng,[‡] Zhaoyu Meng,[‡] Weichao Yu,[‡] Shuyuan Zhang,[†] Xianming Liu,[†] and Yitai Qian^{*,†,‡}

Structural Research Laboratory and Department of Chemistry, University of Science and Technology of China, Hefei, Anhui, 230026, People's Republic of China

Received August 23, 2002. Revised Manuscript Received February 5, 2003

Multiwall boron nitride nanotubes (BNNTs) were produced with a yield of about 50% by co-pyrolyzing NH_4BF_4 , KBH_4 , and NaN_3 in a temperature range from 450 to 600 °C. The obtained BNNTs have a diameter range of 60–350 nm and length range of 0.5–5 μm . Many BN nanocages were found coexisting with the BNNTs. The experimental results indicated that NH_4BF_4 plays a crucial role in the formation of BN nanotubes. The effects of other reactants were also investigated.

Introduction

The discovery of carbon nanotubes in 1991¹ has initiated intensive research activity in the area of nanotubular structures with materials exhibiting a layered structure analogous to graphite, that is, $\text{B}_x\text{C}_y\text{N}_z$,² WS_2 ,³ and MoS_2 .⁴ Hexagonal boron nitride (h-BN) consists of a regular stacking of BN honeycomb sp^2 -like bonded layers very similar to graphite and has almost identical cell parameters ($a = 2.504 \text{ \AA}$; $c = 6.660 \text{ \AA}$) to that of graphite ($a = 2.464 \text{ \AA}$; $c = 6.708 \text{ \AA}$).⁵ BN nanotubes are predicted to be semiconductors with a uniform large gap [roughly 5.5 eV, versus 5.8 eV for bulk hexagonal BN]⁶ regardless of tube diameter, chirality, or the number of tube walls,⁷ which are highly promising for the creation of nanoscale electronic devices and nanostructured ceramic materials, as hydrogen storage materials⁸ and as protective shields for encapsulated species.⁹ Various methods have been used for the preparation of BN nanotubes, namely, by arc discharge,¹⁰ chemical vapor deposition (CVD),¹¹ laser abla-

tion,¹² ball-milling,¹³ carbon-thermal reduction method,¹⁴ carbon nanotube- and template-confined methods,¹⁵ and pyrolysis method.¹⁶ BNNTs with high purity were successfully obtained by these methods at temperatures above 750 °C. Among these methods, the pyrolysis method is one of the most effective methods for preparing boron nitride nanotubes, for example: crystalline BN nanotubes have been synthesized by pyrolyzing the precursor borazine ($\text{B}_3\text{N}_3\text{H}_6$) on nickel boride catalyst particles at ~1100 °C;¹⁶ BN with tubular structures were obtained from the thermal treatment of the product of the reaction between $\text{B}_3\text{X}_3\text{N}_3\text{H}_3$ ($\text{X} = \text{C1, Br}$) and alkali metals (Cs, Rb, K) in the absence of a solvent.¹⁷ In this paper, a co-pyrolysis preparation of multiwall BN nanotubes and BN nanocages in autoclaves in a temperature range from 450 to 600 °C was reported. NH_4BF_4 , KBH_4 , and NaN_3 together with a mixture of Zn and Fe (Zn–Fe) powder were successfully used to prepare BNNTs with a yield of about 50%.

Experimental Section

To prevent oxygen contamination, all the manipulations were carried out in a N_2 flowing glovebox. All the reagents used were of analytical-grade purity (purchased from Shanghai Chem. Co.). In a typical experiment procedure, NH_4BF_4 (0.028 mol), KBH_4 (0.025 mol), and NaN_3 (0.020 mol) together with a mixture of Zn powder (0.022 mol) and reduced Fe powder (0.042 mol) were put into a 25-mL stainless steel autoclave.

- * To whom correspondence should be addressed. E-mail: ytqian@ustc.edu.cn or xulq@mail.ustc.edu.cn. Telephone: +86-551-3602942. Fax: +86-551-3607402.
- † Structural Research Laboratory.
- ‡ Department of Chemistry.
- (1) Iijima, S. *Nature* **1991**, *354*, 56.
- (2) Stephan, O.; Ajayan, P. A.; Colliex, C.; Redlich, Ph.; Lambert, J. M.; Bernier, L. P.; Lefin, P. *Science* **1994**, *266*, 1683.
- (3) Tenne, R.; Margulis, L.; Genut, M.; Hodes, G. *Nature* **1992**, *360*, 444.
- (4) Feldman, Y.; Wasserman, E.; Srolovitz, D. J.; Tenne, R. *Science* **1995**, *267*, 222.
- (5) Pease, R. S. *Acta Crystallogr.* **1952**, *5*, 236.
- (6) Zunger, A.; Katzir, A.; Halperin, A. *Acta Crystallogr.* **1976**, *13*, 5560.
- (7) Blase, X.; Rubio, A.; Louie, S. G.; Cohen, M. L. *Europhys. Lett.* **1994**, *28*, 335.
- (8) (a) Ma, R. Z.; Bando, Y.; Zhu, H. W.; Sato, T.; Xu, C. L.; Wu, D. H. *J. Am. Chem. Soc.* **2002**, *124*, 7672. (b) Tang, C. C.; Bando, Y.; Ding, X. X.; Qi, S. R.; Golberg, D.; Sato, T.; *J. Am. Chem. Soc.* **2002**, *124*, 1450.
- (9) (a) Chopra, N. G.; Zettl, A. *Solid State Commun.* **1995**, *105*, 297. (b) Vaccarini, L.; Goze, C.; Henrard, L.; Hernandez, E.; Bernier, P.; Rubio, A. *Carbon* **2001**, *38*, 1681. (c) Srivastava, D.; Menon, M.; Cho, K. *Phys. Rev. B* **2001**, *63*, 195413.
- (10) Chopra, N. G.; Luyken, R. J.; Cherrey, K.; Crespi, V. H.; Cohen, M. L.; Louie, S. G.; Zettl, A. *Science* **1995**, *269*, 966.

- (11) Ma, R.; Bando, Y.; Sato, T. *Adv. Mater.* **2002**, *14*, 366.
- (12) Laude, T.; Matsui, Y.; Marraud, A.; Jouffrey, B. *Appl. Phys. Lett.* **2000**, *76*, 3239.
- (13) Chen, Y.; Gerald, J. F.; Williams, J. S.; Bulcock, S. *Chem. Phys. Lett.* **1999**, *299*, 260.
- (14) Pokropivny, V. V.; Skorokhod, V. V.; Oleinik, G. S.; Kurdyumov, A. V.; Bartnitskaya, T. S. *J. Solid State Chem.* **2000**, *154*, 214.
- (15) (a) Han, W.; Bando, Y.; Kurashima, K.; Sato, T. *Appl. Phys. Lett.* **1998**, *73*, 3085. (b) Shelimov, K. B.; Moskivits, M. *Chem. Mater.* **2000**, *12*, 250.
- (16) Lourie, O. R.; Jones, C. R.; Bartlett, B. M.; Gibbons, P. C.; Ruoff, R. S.; Buhro, W. E. *Chem. Mater.* **2000**, *12*, 1808.
- (17) (a) Hamilton, E. J. M.; Dolan, S. E.; Mann, C. M.; Colijn, H. O.; McDonald, C. A.; Shore, S. G. *Science* **1993**, *260*, 659. (b) Hamilton, E. J. M.; Dolan, S. E.; Mann, C. M.; Colijn, H. O.; Shore, S. *Chem. Mater.* **1995**, *7*, 111.

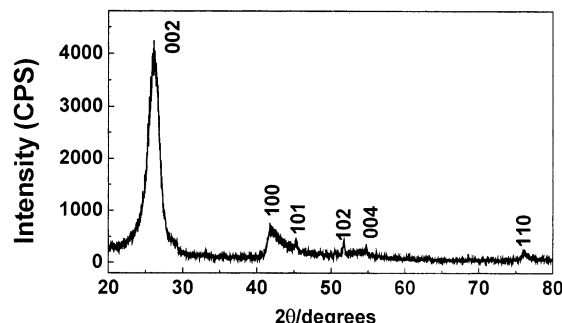


Figure 1. A typical X-ray powder diffraction pattern of the products.

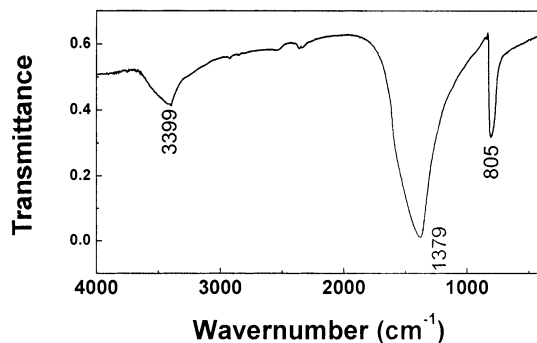


Figure 2. FTIR spectrum of the products.

The autoclave was tightly sealed and heated in an electric stove with an increasing speed of 10 °C/min and maintained in a temperature range from 450 to 600 °C for 40 h, and then it was cooled to room temperature naturally. Although most of the gases produced in the autoclave are exhausted, the autoclave should still be opened carefully. The product in the autoclave was collected and washed with diluted hydrochloric acid and distilled water several times until the solution was neutral. The final product was dried in a vacuum at 70 °C for 3 h.

X-ray powder diffraction (XRD) pattern of the products was recorded on a Japan MXPAHF rotating anode X-ray diffractometer with Cu K α_1 radiation ($\lambda = 1.54056 \text{ \AA}$). Fourier transform infrared (FTIR) spectroscopy of the samples was conducted at room temperature with a KBr pellet on a VECTO-22 (Bruker) spectrometer ranging from 400 to 4000 cm^{-1} . X-ray photoelectron spectroscopy (XPS) measurements were performed on a VGESCALAB MKII X-ray photoelectron spectrometer with an exciting source of Mg K $\alpha = 1253.6 \text{ eV}$. Transmission electron microscopy (TEM) was operated on an Hitachi H-800 transmission electron microscope with an accelerating voltage of 200 kV. The contents of BN nanotubes in the so-prepared products were estimated by statistical analysis of the TEM images. A high-resolution transmission electron microscopy (HRTEM) study was carried out in a JEOL 2010 transmission electron microscope. A Gatan-2000 spectrometer (attached on a JEM-2010F TEM) with a beam energy of 200 kV was used for parallel detection of electron energy loss spectra (EELS).

Results and Discussions

A typical XRD pattern of the obtained products is shown in Figure 1; the reflections can be indexed as hexagonal BN with lattice constants of $a = 2.49 \text{ \AA}$ and $c = 6.67 \text{ \AA}$, which are close to the reported values of h-BN ($a = 2.5044 \text{ \AA}$, $c = 6.6562 \text{ \AA}$) (JCPDS, No. 45-895). No noticeable peaks of impurities were observed in the XRD pattern.

Figure 2 shows a typical FTIR spectrum of the samples. Two strong characteristic peaks locate at 1379 and 805 cm^{-1} , respectively. The absorption band cen-

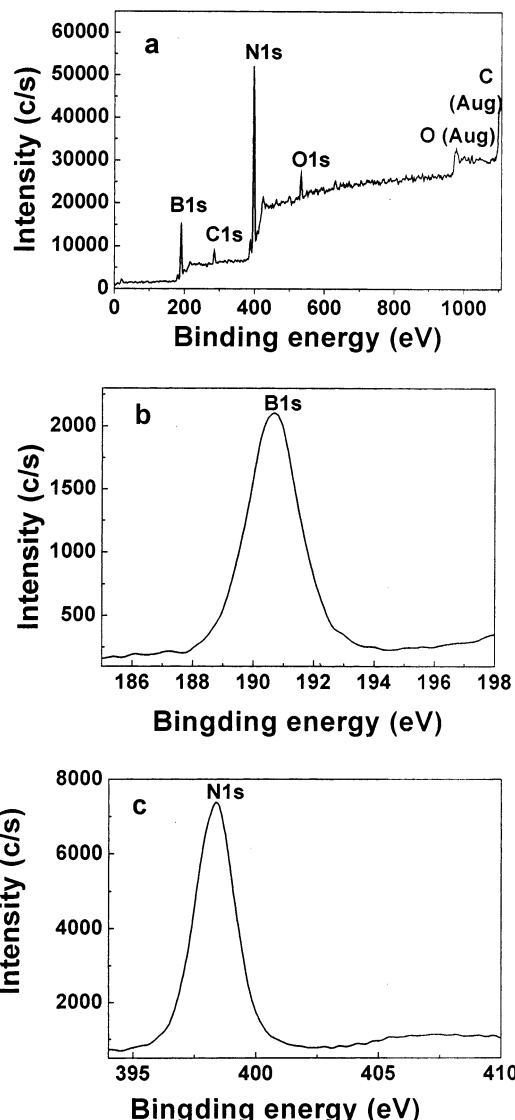


Figure 3. XPS spectra of the products. (a) The survey spectrum; (b) B 1s; (c) N 1s.

tered around 1379 cm^{-1} should be from the in-plane B–N TO modes of the sp^2 -bonded h-BN, and the absorption band at 805 cm^{-1} could be attributed to the B–N–B out-of-plane bending vibration.¹⁸ The broad absorption peak at 3399 cm^{-1} was due to adsorbed water on the samples.

XPS was employed to derive overall compositional information of the obtained products (Figure 3). Figure 3a shows a typical survey spectrum of the products indicating the presence of B and N elements, and the amount of impurities such as CO_2 , H_2O , and O_2 adsorbed on the surface of the samples is small. The binding energies centered at 190.55 eV for B 1s (Figure 3b) and 398.40 eV for N 1s (Figure 3c) are in good agreement with the values of bulk BN in the literature.¹⁹ Quantification of B 1s and N 1s peaks gave an average B:N atomic ratio of 1.05:1. This result, together

(18) Tang, C. C.; Bando, Y.; Sato, T.; Kurashima, K. *Adv. Mater.* **2002**, *14*, 1046.

(19) Wagner, C. D.; Riggs, W. M.; Davis, L. E.; Moulder, J. F.; Muilenberg, G. E., Ed.; *Handbook of X-ray Photoelectron Spectroscopy*; Perkin-Elmer Corporation, Physical Electronics Division: Eden Prairie, Minnesota, 1979.

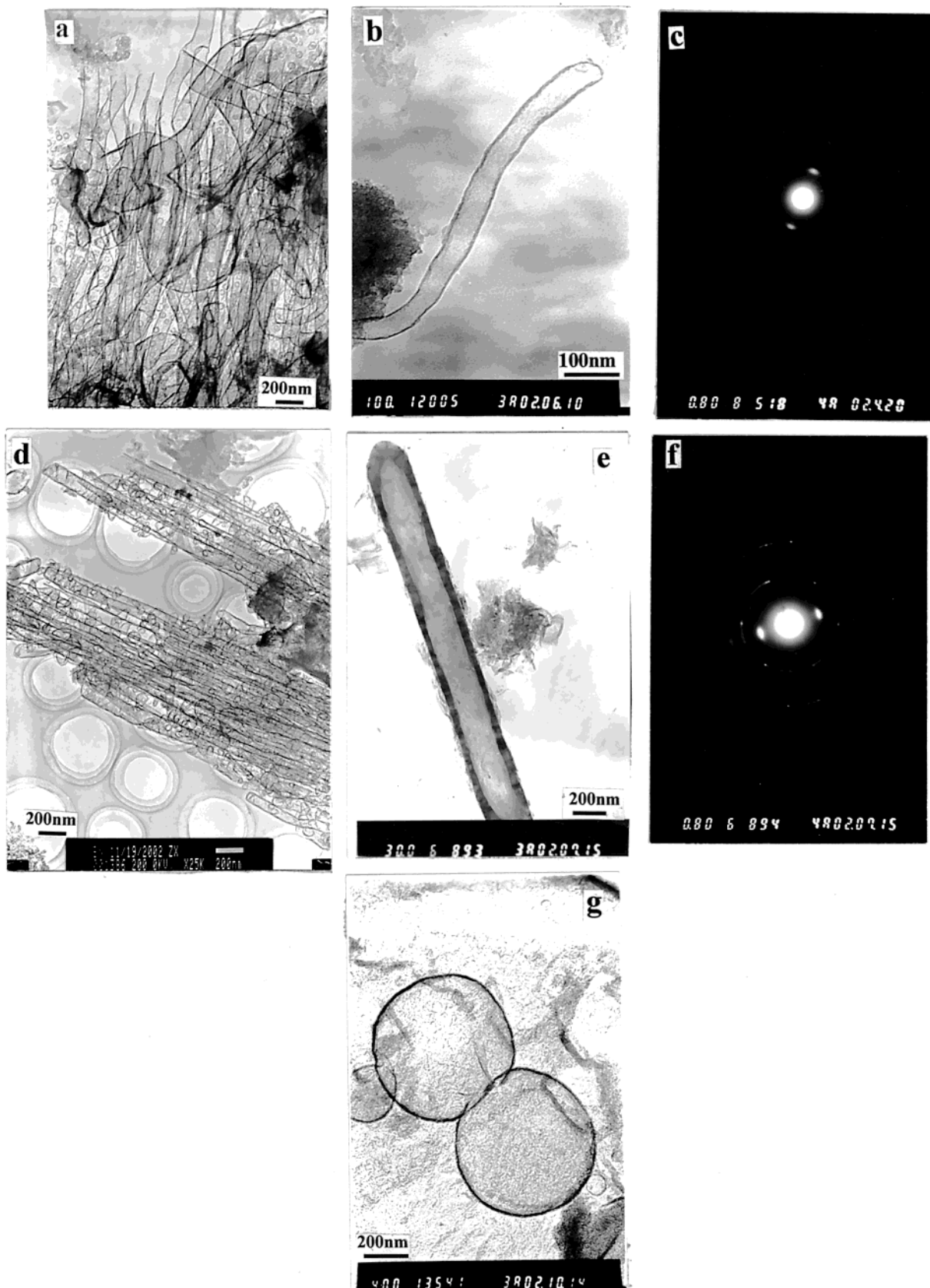


Figure 4. Representative TEM images of the BN nanotubes, nanocages prepared at 450 and 600 °C. (a) and (b) show the BN nanotubes and nanocages prepared at 450 °C. (c) A typical ED pattern of a single BN nanotube shown in (a). (d) and (e) show the BN nanotubes and nanocages prepared at 600 °C. (f) The ED pattern of the nanotube shown in (e). (g) A typical TEM image of the BN nanocages.

with the above analyses, confirmed that the products were h-BN.

TEM observation indicated that the so-prepared products were mainly composed of BN nanotubes,

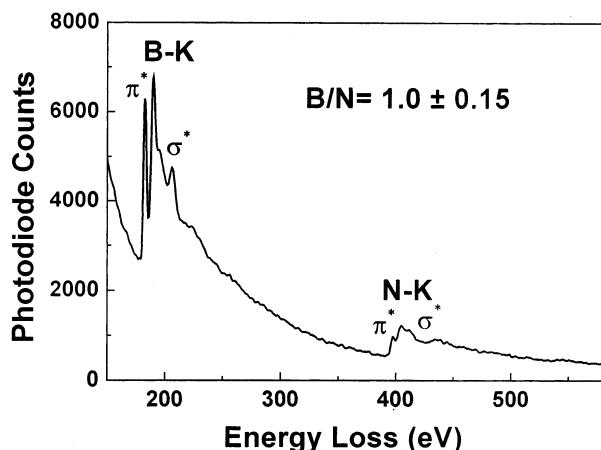


Figure 5. Typical electron energy loss spectrum (EELS) of one BN nanotubes; only the B and N K-edge can be observed.

nanocages, and turbostratic h-BN,¹⁷ and the yield of BNNTs was about 50%. Figure 4 shows representative TEM images and typical ED patterns of the BNNTs obtained at 450 °C (Figure 4a–c) and at 600 °C (Figure 4d–g). The present BN nanotubes have a diameter range of 60–350 nm, which is larger than that of the BNNTs previously reported,^{10,20} and the length of the BNNTs varies from 0.5 to 5 μ m. Comparing the TEM images of the BNNTs prepared at 450 °C with those prepared at 600 °C, it can be seen that the BNNTs prepared at 600 °C (Figure 4d,e) are straighter and more uniform than the BNNTs (Figure 4a,b) prepared at 450 °C. The crystallinity of the BNNTs prepared at 600 °C (Figure 4c) is better than those prepared at 450 °C (Figure 4f), as was proved by their ED patterns. Besides the BNNTs, many hollow nanocages²¹ (Figure 4a,d,g) are observed coexisting with the BN nanotubes. A representative EELS spectrum taken from a single BN nanotube is shown in Figure 5. Two distinct absorption features are observed at 190 and 404 eV, which correspond to boron K-edge and nitrogen K-edge, respectively. Quantification of the EELS spectrum gave a B/N atomic ratio of 1.0 ± 0.15 . The sharp π^* -peaks on the left side of the B and N K-edges and the shapes of the σ^* -bands on the right side confirmed that the tubular layers were composed of sp^2 -bonded B and N atoms.²²

It was found that the so-prepared BNNTs with closed ends had various tips. Most of the enclosed BN nanotubes possess conelike tips with an acute angle (Figure 6a) or possess obtuse tips, while squarelike tips with a nearly right angle (Figure 6b) were occasionally encountered. A high-resolution TEM image of a corner of the squarelike tip (as arrowed) is shown in Figure 6c, and the average distance between the neighboring fringes is about 0.34 nm, which is consistent with the interplanar distance of 0.333 nm in bulk h-BN.²³ It was thought that the various kinds of tips were probably caused by topological defects as suggested by Golberg and Bando.²⁴

(20) (a) Ma, R.; Bando, Y.; Sato, T.; Kurashima, K. *Chem. Phys. Lett.* **2001**, *350*, 434. (b) Tang, C. C.; Ding, X. X.; Huang, X. T.; Gan, Z. W.; Qi, S. R.; Liu, W.; Fan, S. S. *Chem. Phys. Lett.* **2002**, *356*, 254.

(21) Golberg, D.; Bando, Y.; Stephan, O.; Kurashima, K. *Appl. Phys. Lett.* **1998**, *73*, 2441.

(22) Bando, Y.; Ogawa, K.; Golberg, D. *Chem. Phys. Lett.* **2001**, *347*, 349.

(23) Paine, R. T.; Narula, C. K. *Chem. Rev.* **1990**, *90*, 73.

The reactions involved in our experiment are fairly complex; to study the effects of the reactants on the formation and yield of BN nanotubes, a series of experiments were carried out (as shown in Table 1) with the procedure similar to that mentioned in the Experimental Section. The experiments shown in Table 1 were divided into 5 groups according to the different boron and nitrogen sources and each group contains 4 reactions. The 4 reactions were arranged in sequence of (1) without metal powder, (2) with Zn powder only, (3) with Fe powder only, and (4) with Zn–Fe bi-metal powder. The overall experimental results shown in Table 1 indicate that $NaBF_4$ was necessary for the production of h-BN; without $NaBF_4$, no BN could be obtained. This is particularly supported by the results of group 1. Group 2 indicates that h-BN can be obtained with very low yield just using $NaBF_4$ as reactant, and the yield of h-BN can be increased a little when Zn or Fe powder was added, but the products did not contain BNNTs. However, $NaBF_4$ can react with Zn–Fe bi-metal powder to produce a small amount of BNNTs, which shows that Zn and Fe powder have a synergic effect on the formation of BNNTs (as can be seen from groups 2, 3, 4, and 5). When NaN_3 was added into the reactants of the corresponding reactions of group 2, we obtained group 3; group 3 indicated that the contents of BNNTs were increased quite a bit compared with those of group 2, while the yields of h-BN varied greatly. For example, h-BN with high yield was obtained when Zn or Zn–Fe powders were used. When KBH_4 was added into the reactants of group 2, we obtained group 4. The results indicated that the addition of KBH_4 could increase the total yield of h-BN and the contents of BNNTs, but the contents of BNNTs were still lower than those of group 3. It can be seen from group 3 and group 4 that Zn powder has a more active effect than Fe powder in increasing the yield of BNNTs. Although the results of group 3 and group 4 might give one an impression that KBH_4 was important for the production of h-BN and NaN_3 for the production of BNNTs, we cannot reach a conclusion that KBH_4 was not important for the formation of BNNTs. When KBH_4 and NaN_3 were added into the reactants of group 2 simultaneously, we obtained group 5. It can be seen that the total yield of h-BN and the contents of BNNTs were both greatly increased, which shows that KBH_4 and NaN_3 also have a synergic effect in the production of BNNTs. The experimental results that the highest contents of BNNTs in each group (groups 2, 3, 4, and 5) were obtained only when Zn and Fe powder were added simultaneously were impressive and further prove the synergic effect of Zn–Fe bi-metal powder. On the basis of Table 1, we tentatively think that Zn and Fe powder used in this experiment have a quasi-catalyst function (as can be seen from groups 2, 3, 4, and 5) in the formation of BN nanotubes.²⁵ This point of view is partly supported by the work of Higashi and co-workers, who found that elemental zinc can react with boron trichloride even below 1000 °C to form no stable borides with boron,²⁶ and by the work of Lourie et al., who prepared multiwall BNNTs by a CVD method using Co, Ni, NiB, and Ni_2B

(24) Golberg, D.; Bando, Y. *Appl. Phys. Lett.* **2001**, *79*, 415.

(25) Chen, Y.; Chadderton, L. T.; Gerald, J. F.; Williams, J. S. *Appl. Phys. Lett.* **1999**, *74*, 2960.

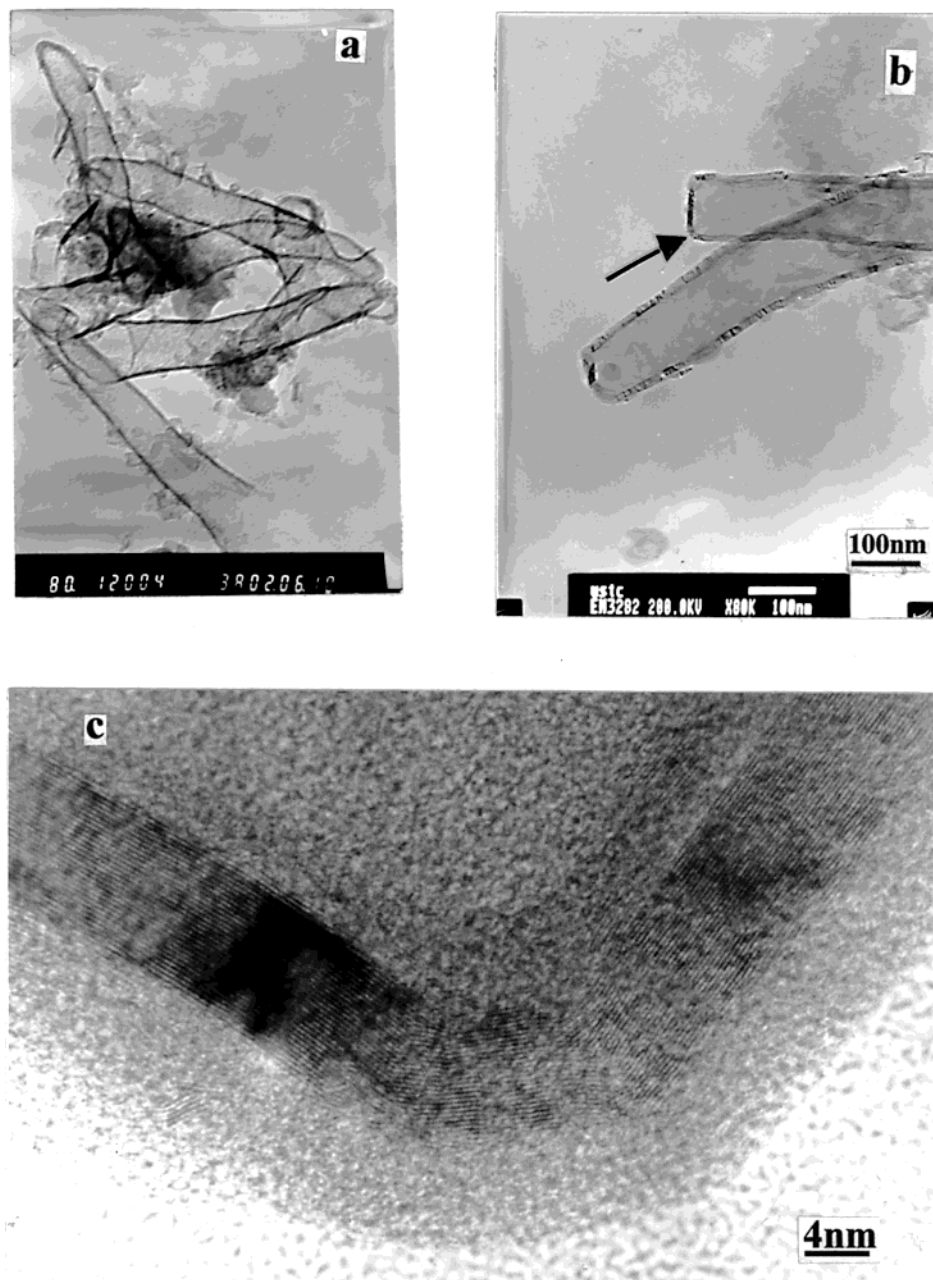
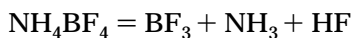


Figure 6. TEM images of the BNNTs with conelike tips and squarelike tips prepared at 450 °C and a HRTEM image of a corner of a squarelike tip. (a) BNNTs with conelike tips. (b) BNNTs with squarelike tips. (c) HRTEM image of a corner (arrowed) of a squarelike tip in (b).

particulate catalysts at ~1100 °C.¹⁶ As there are so many reactants involved in the reactions of the present experiment, we cannot clarify the exact reaction mechanism for the time being, but we are sure that NH₄BF₄ must decompose to initialize the reaction, as can be seen from Table 1, which can be written as the following equation:²⁷



It is worth noting that irregular BN nanotubes (see Figure 4a,b), BNNTs with conelike or squarelike tips (see Figure 6a,b), and BN nanocages (see Figure 4h) widely existed in the so-prepared samples. According to the previous reports that ring (topology) defects are necessary to the emergence of curvature in layered structures on the nanometric scale, and an ordered

arrangement of some specific ring defects within a hexagonal lattice would lead to closed cage structures,²⁸ we consider that the irregular BNNTs, the conelike and squarelike tips, and the nanocages may be caused by topological defects too, which is similar to the formation mechanism of carbon, MoS₂, and WS₂ nanotubes.²⁹ Since it is energetically unfavorable to have topological

(26) (a) Higashi, K. *Kyushu Kozan Gakkai-Shi* **1961**, 29, 312. (b) *Chem. Abstr.* **1961**, 26, 807. (c) Higashi, K. *Kyushu Kozan Gakkai-Shi* **1962**, 29, 209. (d) *Chem. Abstr.* **1962**, 56, 163. (e) Picon, M.; Pichat, P.; Cueilleron, J. *Compt. Rend. C* **1964**, 258, 5877.

(27) Göbbels, D.; Meyer, G. *Z. Anorg. Allg. Chem.* **2002**, 628, 1799.

(28) Terrones, M.; Hsu, W. K.; Kroto, H. W.; Walton, D. R. M. *Top. Curr. Chem.* **1999**, 199, 189.

(29) (a) Nardelli, M. B.; Fattebert, J.-L.; Orlikowski, D.; Roland, C.; Zhao, Q.; Bernholc, J. *Carbon* **2000**, 38, 1703. (b) Seifert, G.; Terrones, H.; Terrones, M.; Jungnickel, G.; Frauenheim, T. *Phys. Rev. Lett.* **2000**, 85, 146. (c) Margulis, L.; Salitra, G.; Tenne, R. *Nature* **1993**, 365, 113. (c) Kobayashi, K. *Phys. Rev. B* **2000**, 61, 8496.

Table 1. Different Yields of h-BN and Contents of BNNTs Obtained by the Following Experiments Prepared at 600 °C for 40 h

group number	reactant	approximate contents of BNNTs	yield of h-BN
1	KBH ₄ , NaN ₃		
	KBH ₄ , NaN ₃ , and Zn		very low
	KBH ₄ , NaN ₃ , and Fe		low
	KBH ₄ , NaN ₃ and Zn, Fe		low
2	NH ₄ BF ₄		very low
	NH ₄ BF ₄ and Zn	~1%	low
	NH ₄ BF ₄ and Fe		low
	NH ₄ BF ₄ and Zn, Fe		low
3	NH ₄ BF ₄ , NaN ₃	1–2%	very high
	NH ₄ BF ₄ , NaN ₃ , and Zn	5–10%	high
	NH ₄ BF ₄ , NaN ₃ , and Fe	3–5%	very low
	NH ₄ BF ₄ , NaN ₃ and Zn, Fe	15–20%	high
4	NH ₄ BF ₄ , KBH ₄	1–2%	high
	NH ₄ BF ₄ , KBH ₄ , and Zn	3–5%	high
	NH ₄ BF ₄ , KBH ₄ , and Fe	1–3%	low
	NH ₄ BF ₄ , KBH ₄ and Zn, Fe	5–7%	high
5	NH ₄ BF ₄ , KBH ₄ , NaN ₃	2–7%	high
	NH ₄ BF ₄ , KBH ₄ , NaN ₃ , and Zn	10–15%	high
	NH ₄ BF ₄ , KBH ₄ , NaN ₃ , and Fe	15–25%	high
	NH ₄ BF ₄ , KBH ₄ , NaN ₃ and Zn, Fe	~50%	high

defect rings with B–B or N–N bonds, only even-numbered defect rings (for example, four- and eight-membered rings) are possible to exist and are responsible for the formation of the obtuse and squarelike tips.^{10,28} Topological defects may be produced for various reasons;³⁰ in this experiment, the topological defects

might be produced by the etching ability of HF and BF₃ molecules, or even by some F-containing free radicals. Of course, due to the complexity of the present experiment, the exact formation mechanism of the BNNTs and nanocages still needs further research.

Conclusions

In summary, NH₄BF₄, KBH₄, and NaN₃ together with a mixture of Zn powder and reduced Fe powder were successfully used for the synthesis of multiwall BN nanotubes and nanocages in a temperature range from 450 to 600 °C. BNNTs with a diameter range of 60–350 nm and length range of 0.5–5 μm were produced with relatively high yield (about 50%). Enclosed BNNTs with different tips, like acute, obtuse, and square tips, were observed in this experiment and many BN nanocages were found coexisting with the BNNTs. The experimental results indicate that NH₄BF₄ plays a crucial role in the formation of BNNTs; the use of KBH₄ and NaN₃ can increase both the yield of the h-BN and the contents of BNNTs. In addition, Zn and Fe powder might play a quasi-catalytic role in the formation of BNNTs.

Acknowledgment. We acknowledge the financial support from the 973 Climbing Project Foundation of China.

CM020853L

(30) (a) Tamura, R.; Akagi, K.; Tsukada, M.; Itoh, S.; Thara, S. *Phys. Rev. B* **1997**, *56*, 1404. (b) Bettinger, H. F.; Dumitrica, T.; Scuseria, G. E.; Yakobson, B. I. *Phys. Rev. B* **2002**, *65*, 041406.